Article ID: 1006-8775(2021) 01-0062-08

Retrieval of Sea Surface Wind Speed by One-Dimensional Synthetic Aperture Microwave Radiometer

AI Wei-hua (艾未华)[1], FENG Meng-yan (冯梦延)[1], LU Wen (陆 文)[1], MA Shuo (马 烁)[1], CHEN Guan-yu (陈冠宇)[2]
(1. College of Meteorology and Oceanography, National University of Defense Technology, Nanjing 211101 China; 2. PLA Troop 32033, Haikou 570100 China)

Abstract: One-dimensional synthetic aperture microwave radiometers have higher spatial resolution and record measurements at multiple incidence angles. In this paper, we propose a multiple linear regression method to retrieve sea surface wind speed at an incidence angle between 0° ~65° . We assume that a one-dimensional synthetic aperture microwave radiometer operates at frequencies of 6.9, 10.65, 18.7, 23.8 and 36.5 GHz. Then, the microwave radiative transfer forward model is used to simulate the measured brightness temperatures. The sensitivity of the brightness temperatures at 0°~65° to the sea surface wind speed is calculated. Then, vertical polarization channels (VR), horizontal polarization channels (HR) and all channels (AR) are used to retrieve the sea surface wind speed via a multiple linear regression algorithm at 0° ~65° , and the relationship between the retrieval error and incidence angle is obtained. The results are as follows: (1) The sensitivity of the vertical polarization brightness temperature to the sea surface wind speed is smaller than that of the horizontal polarization. (2) The retrieval error increases with Gaussian noise. The retrieval error of VR first increases and then decreases with increasing incidence angle, the retrieval error of HR gradually decreases with increasing incidence angle, and the retrieval error of AR first decreases and then increases with increasing incidence angle. (3) The retrieval error of AR is the lowest and it is necessary to retrieve the sea surface wind speed at a larger incidence angle for AR.

Key words: sea surface wind speed; high spatial resolution; synthetic aperture microwave radiometer; multiple incidence angles; multiple linear regression algorithm
CLC number: P407.7 **Document code:** A
https://doi.org/10.46267/j.1006-8775.2021.006

1 INTRODUCTION

Sea surface wind speed (SSWS) is an important geophysical parameter that affects ocean dynamic cycles and sea-air interactions (Meissner and Wentz[1]; Yao et al.[2]; Fang et al. [3]). At present, satellite-borne microwave remote sensing has become the main method of SSWS detection (Wang et al.[4]).

The SSWS will affect the sea surface emissivity (Wu and Fung[5]; Wentz[6, 7]; Meissner and Wentz[8]), resulting in changes to the radiation brightness temperature and thus allowing for a microwave radiometer to retrieve the SSWS (Hong and Shin[9]). Compared with real aperture microwave radiometers, one-dimensional synthetic aperture microwave radiometers use a small-aperture antenna array instead of a large real-aperture antenna, and the spatial resolution is determined by spectrum sampling, not by the size of antennas (Vine et al.[10]; Vine[11]; Li et al.[12]). Thus, one-dimensional synthetic aperture microwave radiometer can provide remote-sensing images at a higher spatial resolution than those from traditional real aperture microwave radiometers (Schanda[13]; Ruf et al.[14]; Chen et al.[15]). The concept of one-dimensional synthetic aperture microwave radiometer is shown in Fig. 1. Spaceborne one-dimensional synthetic aperture microwave radiometer can generate a two-dimensional image from a space platform movement (Feng et al.[16]). It scans through a certain angular range with respect to the forward direction of the satellite, with each observation point corresponding to a different incidence angle (Li et al.[17]).

Due to one-dimensional synthetic aperture microwave radiometer has higher resolution, it will be widely used on satellite platform to monitor extreme weather such as tropical cyclones in the future. However, one-dimensional synthetic aperture microwave radiometer has multiple continuous incidence angles which considerably influence the brightness temperature, so the SSWS cannot be retrieved at multiple incidence angles using the retrieval algorithms developed for real-aperture microwave radiometers. Therefore, it is necessary to retrieve SSWS at each incidence angle (i.e., 0°, 1°, 2°, 3°, etc.).

Submitted 2020-06-10; **Revised** 2020-11-15; **Accepted** 2021-02-15
Funding: National Natural Science Foundation of China (41475019, 41631072)
Biography: AI Wei-hua, Associate Professor, primarily undertaking research on radar and radiometer.
Corresponding author: FENG Meng-yan, e-mail: a1044175130@163.com

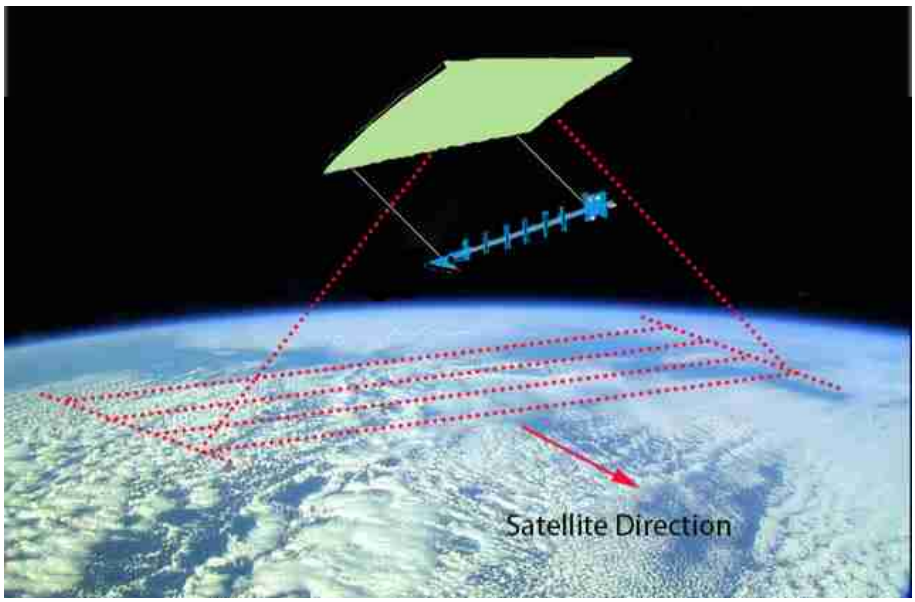

Figure 1. Schematic diagram of the scan process of a one-dimensional synthetic aperture microwave radiometer.

At present, the sea surface wind speed retrieval algorithms for microwave radiometer mainly include physical algorithms (Ai et al.[18]; Bettenhausen et al.[19]; Brown et al.[20]; Koner et al.[21]; Meissner and Wentz[22]) and empirical algorithms (Wentz and Meissner[23]; Goodberlet et al.[24]; Obligis et al.[25]; Krasnopolsky et al.[26]; An et al.[27]; Jena et al.[28]; Alsweiss et al.[29]; Wang et al.[30]; Smith et al.[31]). The physical algorithms are based on the radiative transfer model, which retrieves sea surface SSWS by establishing a cost function of observations and model simulations. However, the physical retrieval algorithms require a large amount of computing resources, so we propose a multiple linear regression algorithm for one-dimensional synthetic aperture microwave radiometer to retrieve the SSWS from space. The algorithm involves a small amount of computing resources and is easy to implement, so it can be used as an on-board processing method in the future. In addition, we study the retrieval results and the sensitivity to the SSWS based on simulation in the range of 0°~ 65°.

The rest of this paper is organized as follows. The proposed retrieval algorithm and the forward model are presented in section 2. The results and discussion are introduced in section 3. The conclusions are presented in section 4.

2 METHODOLOGY

In this paper, we use the frequency of WindSat as a reference to assume a one-dimensional synthetic aperture microwave radiometer which operate at frequencies of 6.9, 10.65, 18.7, 23.8, and 36.5 GHz. All frequencies work in a dual polarization manner (vertical and horizontal polarization). We used vertical polarization channels (VR), horizontal polarization channels (HR) and all channels (AR) to retrieve the SSWS via a multiple linear regression algorithm, respectively. Fig. 2 shows the process of retrieving the SSWS.

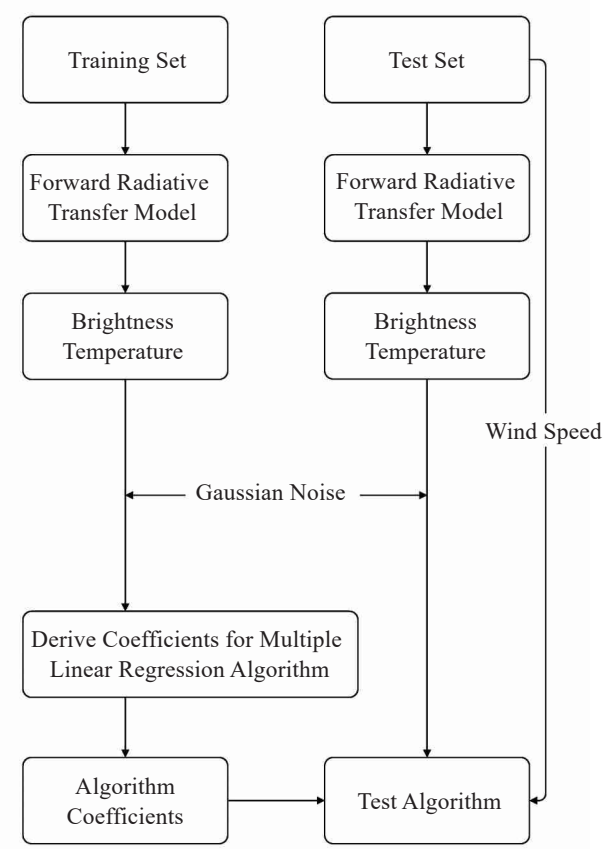

Figure 2. Diagram of the process of retrieving the SSWS.

2.1 *Retrieval method*

The multiple linear regression equation is as follows (Wilheit and Change[32]; Lojou et al.[33]; Milman and Wilheit[34]):

$$W=R\left[A_0+\sum_{i=1}^{n}A_i\cdot X\left(T_{B,\mathrm{meas},i}^{\theta}\right)\right] \quad (1)$$

where W is the *SSWS*, R and X are linearizing functions, A_i is the regression coefficients, n is the number of channels, and $T_{B,\mathrm{meas},i}^{\theta}$ is the brightness temperature measured by a spaceborne one-dimensional synthetic aperture microwave radiometer.

In this paper, we use the following linearization functions:

$$R(F)=F$$

$$X(T_B)=T_B \qquad f=6.9 \text{ and } 10.65 \text{ GHz}$$

$$X(T_B)=-\ln(290-T_B) \qquad f=18.7, 23.8, \text{and } 36.5 \text{ GHz}$$

2.2 *Data*

As shown in Fig. 2, radiation transmission forward model and environmental scenes are crucial for deriving regression coefficients and verifying the feasibility of this algorithm. In this paper, the newest version of the European Centre for Medium-Range Weather Forecasts (ECMWF) reanalysis data, ERA5(Li et al.[35]), is used to establish environmental scenes. The data contain the 10-m wind speed components u and v, the total column cloud liquid water content L, the total column water vapour content V, the average rainfall rate R and the sea surface temperature T_S. The acquisition times are 0:00 and 12:00 on January 15, April 15, July 15, and October 15, 2018. The spatial resolution of the data is 0.25°. The wind speed W and wind direction φ are calculated by using the 10-m wind speed components u and v. Data with $R>0$, $T_S<271.15$ and $L<0$ are eliminated, resulting in approximately 710,000 sets of data after processing. The seawater salinity S is set to 35 psu because S has little effect on the frequencies of the one-dimensional synthetic aperture microwave radiometer.

We obtain approximately 730,000 sets of data after processing. Statistical histograms of the sea surface temperature, wind direction, wind speed, total column cloud liquid water content and total column water vapour content are shown in Fig. 3. Finally, we randomly divide the data into a training set and a test set on average. The training set is used to train the retrieval algorithm, and the test set is used to test its performance.

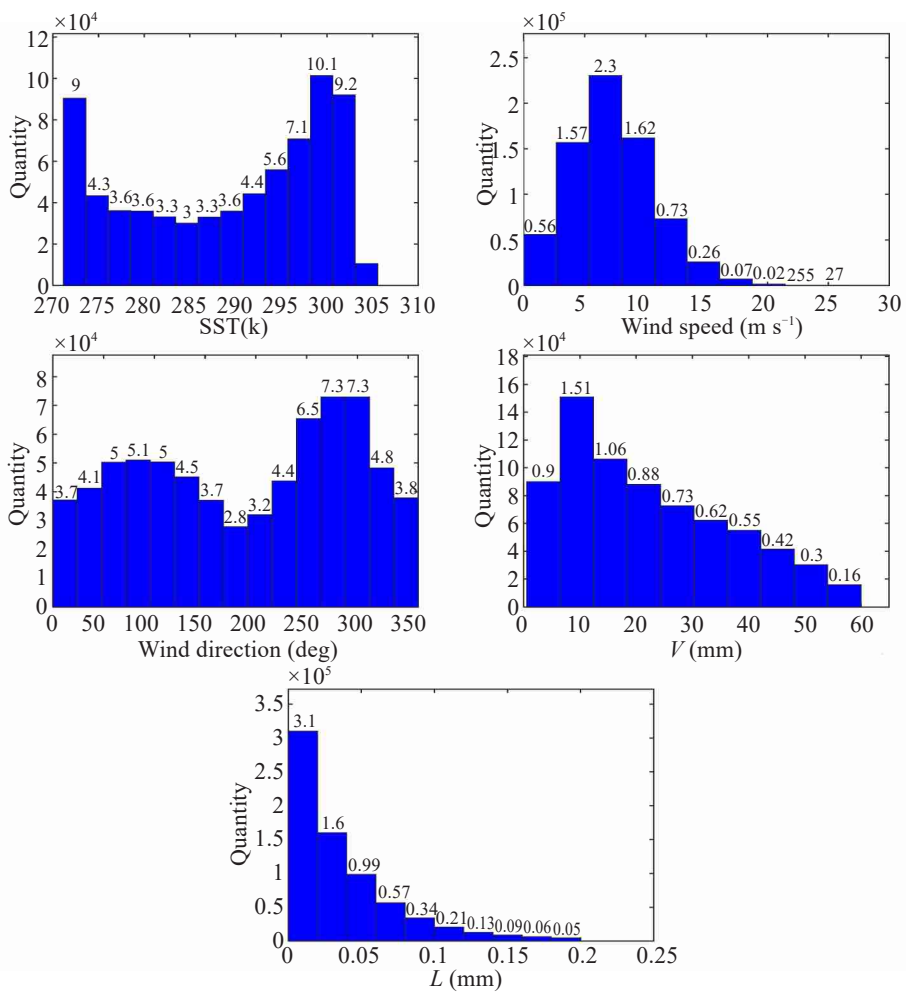

Figure 3. Distribution histograms of environmental parameters: (a) sea surface temperature, (b) SSWS, (c) sea surface wind direction, (d) total column cloud water vapour content, and (e) total column cloud liquid water content.

2.3 *Ocean-atmospheric radiation transmission forward model*

According to the theory of polarized radiative transfer (Hilburn et al.[36]; Meissner and Wentz[1,7]), the brightness temperature $T^{\theta}_{B,\mathrm{mod},p}$ which is theoretically received by the spaceborne one-dimensional synthetic aperture microwave radiometer can be expressed as follows:

$$\begin{aligned} T^{\theta}_{B,\mathrm{mod},p} &= T_{BU,\theta} + \tau_{\theta} \cdot E_{p,\theta} \cdot T_S + \tau_{\theta} \cdot T_{B\Omega,\theta} \\ T_{B\Omega,\theta} &= R_{p,\theta} \cdot [T_{BD,\theta} + \tau_{\theta} \cdot T_{\mathrm{cold}}] + T_{B,\mathrm{scat},p,\theta} \end{aligned} \tag{2}$$

where the subscript θ denotes the incidence angle, $0° \leqslant \theta \leqslant 65°$; the subscript p denotes the polarization mode, $p = v, h$; $T_{BU,\theta}$ and $T_{BD,\theta}$ are the upwelling and downwelling atmospheric brightness temperatures, respectively; τ_{θ} is the atmospheric transmittance; $E_{p,\theta}$ is the total sea surface emissivity; T_S is the sea surface temperature; $T_{B\Omega,\theta}$ is the downwelling sky radiation that is scattered from the sea surface; $R_{p,\theta} = 1 - E_{p,\theta}$ is the sea surface reflectivity; T_{cold}=2.7K is the effective cold space temperature. $\tau_{\theta} \cdot T_{B,\mathrm{scat},p,\theta}$ represents the atmospheric path length correction for the downwelling scattered sky radiation.

The forward model of microwave radiative transfer is divided into components related to atmospheric radiation and ocean radiation. We use the sea surface emissivity model developed by Meissner and Wentz[7] in 2012:

$$E_{p,\theta} = E_{0,p,\theta} + \Delta E_{W,p,\theta} + \Delta E_{\varphi,p,\theta} \tag{3}$$

where $E_{0,p,\theta}$ is the specular sea surface emissivity, which is a function of the frequency f, incidence angle θ, sea surface temperature T_S and salinity S and can be calculated using Fresnel's law (Meissner and Wentz[7, 37]); $\Delta E_{W,p,\theta}$ is the emissivity increase caused by the wind speed W; $\Delta E_{\varphi,p,\theta}$ represents the four Stokes parameters of the sea surface wind direction signal and captures the dependence on the wind direction φ.

$\Delta E_{W,p,\theta}$ is used as the basis for the retrieval of the SSWS, and it is a function of the frequency f, SSWS W, incidence angle θ, sea surface temperature T_S and salinity S. $\Delta E_{W,p,\theta}$ can be expressed as follows (Meissner and Wentz[7]):

$$\Delta E_{W,p,\theta}(\theta, W, T_S, S) = \Delta E_{W,\mathrm{nad}}(W, T_S, S) + [\Delta E_{W,p,\theta}(\theta, W, T_S, S) - \Delta E_{W,\mathrm{nad}}(W, T_S, S)] \cdot \left(\frac{\theta}{\theta_{\mathrm{ref}}}\right)^{x_p}, \tag{4}$$

$$\Delta E_{W,\mathrm{nad}}(W, T_S, S) = \frac{1}{2}[\Delta E_{W,v}(\theta_{\mathrm{ref}}, W, T_S, S) + \Delta E_{W,h}(\theta_{\mathrm{ref}}, W, T_S, S)], \tag{5}$$

$$\Delta E_{W,p}(\theta_{\mathrm{ref}}, W, T_S, S) = \delta_{\mathrm{ref},p}(W) \cdot \frac{E_{0,p}(\theta_{\mathrm{ref}}, T_S, S)}{E_{0,p}(\theta_{\mathrm{ref}}, T_{\mathrm{ref}}, S)}, \tag{6}$$

$$\delta_{\mathrm{ref},p}(W) = \sum_{k=1}^{5} \delta_{k,p} \cdot W^k, \tag{7}$$

where x_p represents x_v=4.0 and x_H=1.5, the subscript nad denotes the satellite nadir angle, $\theta_{\mathrm{ref}} = 55.2°$ is the reference incidence angle, $T_{\mathrm{ref}} = 20°C$ is the reference temperature, and $\delta_{k,p}$ is the interpolation coefficient, which is related to the wind speed.

Scattering can be neglected under non-precipitating atmospheric conditions (Meissner and Wentz[7]). In the frequency range below 100 GHz, the main absorptive components of the atmosphere are oxygen, water vapour and liquid water, $T_{BU,\theta}$, $T_{BD,\theta}$ and τ_{θ} can be calculated from the atmospheric profile (Wentz and Meissner[23]; Waters[38]). Considering the amount of computation required and the size of the data, we use an empirical model to calculate $T_{BU,\theta}$, $T_{BD,\theta}$ and τ_{θ}(Wentz and Meissner[23]; Waters[38]). The empirical model requires the frequency f, incidence angle θ, sea surface temperature T_S, total column liquid water content L, and total column water vapour content V as inputs. It should be noted that Equation (8) is adopted in this paper to calculate the absorption coefficient of liquid water A_L (Rui et al.[39]) because the empirical model requires the average cloud temperature T_L as an input, which is difficult to obtain.

$$A_L = b_{L0}(1 + b_{L1}V)L \tag{8}$$

where A_L is the absorption coefficient of liquid water, V is the total column water vapour content, L is the total column liquid water content, b_{L0} and b_{L1} are the regression coefficients.

We use the radiation transmission model to calculate the modelled brightness temperature $T^{\theta}_{B,\mathrm{mod},p}$, and the measured brightness temperature $T^{\theta}_{B,\mathrm{meas},p}$ was simulated by the sum of a $T^{\theta}_{B,\mathrm{mod},p}$ and the Gaussian noises generated by a random number generator. The Gaussian noise represents an error of the brightness temperature measurement. The average value of the Gaussian noise is 0 K, and standard deviations of 0.2 K, 0.4 K, and 0.6 K are considered. Many researchers use Gaussian noise to simulate measured brightness temperatures (Wentz and Meissner[23]; Bobylev et al.[40]); this is a reasonable approach for preliminary research in the absence of real satellite observation data. It should be noted that the modelling error and the impact of Radio Frequency Interference (RFI) are not considered in this study.

3 RESULT AND DISCUSSION

3.1 *Sensitivity of brightness temperature at five frequencies to SSWS*

Sensitivity of the brightness temperature to the SSWS affects the SSWS retrieval accuracy.

Theoretically, the greater this sensitivity is, the more information on the SSWS is contained in the brightness temperature, and the higher the retrieval accuracy will be. In addition, the interaction between different frequencies during the SSWS retrieval can also affect the SSWS retrieval accuracy, which is difficult to predict. We assume a particular environmental scene to calculate the sensitivity of the brightness temperature at five frequencies to the SSWS, as shown in Table 1.

Table 1. Environmental scene.

Scene	S (psu)	T_S (K)	W (m s^{-1})	φ (°)	V (mm)	L (mm)
Scene 1	35	293	0~30	45	30	0.1

The sensitivity of the brightness temperature to the SSWS at different incidence angles can be calculated using Equation (9):

$$Se_p = \frac{1}{n} \cdot \sum_{i=1}^{n} \left| \frac{\partial T^{\theta}_{B,\mathrm{mod},p}}{\partial W_i} \right|, \tag{9}$$

where Se_p is the average value of the sensitivity of the brightness temperature to the SSWS at an incidence angle of θ, $n = 30$ is the number of SSWS, $T_{B,\mathrm{mod},p,\theta}$ is the mode brightness temperature calculated using the forward model of microwave radiative transfer at an incidence angle of θ, $p = v,h$ is the polarization mode, and W is the SSWS.

Figure 4a and 4b shows the average values of the sensitivity of the vertical and horizontal polarization brightness temperatures, respectively, to the SSWS at different incidence angles. The sensitivity of the horizontal polarization brightness temperature to the SSWS is greater than that of the vertical polarization brightness temperature. The sensitivity of the vertical polarization brightness temperature to the SSWS decreases as the incidence angle increases but remains almost unchanged in the range of 0°~30°, which is because the Se_v is not sensitive to the incidence angle in the range of 0°~30°. The 6.9 and 10.65 GHz horizontal polarization brightness temperatures show an increasing sensitivity to the SSWS as the incidence angle increases. At 18.7, 23.8, and 36.5 GHz, the sensitivity of the horizontal polarization brightness temperature to the SSWS first increases and then decreases as the incidence angle increases.

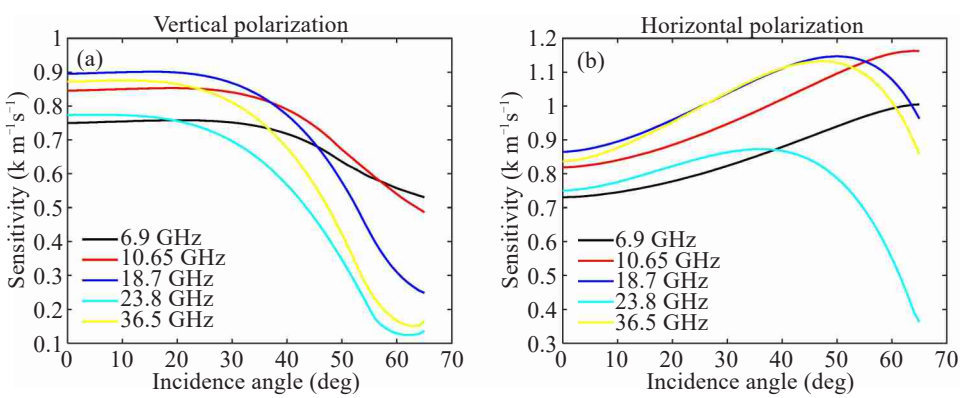

Figure 4. Sensitivity of the brightness temperature to the SSWS as a function of the incidence angle.

3.2 *SSWS retrieval results*

The root-mean-square (RMS) error and mean bias within the range of 0°~65° are calculated in accordance with Equations (10) and (11).

$$\mathrm{RMSE} = \sqrt{\frac{1}{N} \sum_{k=1}^{N} (W_k^{\mathrm{true}} - W_k)^2}, \tag{10}$$

$$\mathrm{RB} = \frac{1}{N} \sum_{k=1}^{N} (W_k^{\mathrm{true}} - W_k), \tag{11}$$

where RMSE is the RMS error, MB is the mean bias, N is the number of samples, W_k^{true} is the true SSWS, and W_k is the retrieved value of the SSWS.

Figure 5 shows the relationships between the RMS error and mean bias and the incidence angle. Fig. 5a and 5b show the retrieval results obtained using only the vertical polarization channels (VR). Fig. 5c and 5d show the retrieval results obtained using only the horizontal polarization channels (HR). Fig. 5e and 5f show the retrieval results obtained using all channels (AR). In each subfigure, the left panel shows the retrieval results for the training set, and the right panel shows the retrieval results for the test set. The results show that the RMS errors on the training and test sets are similar. The mean bias values of VR, HR and AR are very low and fluctuate around 0 m s^{-1}. The black, red and blue lines represent the retrieval results for Gaussian noise with standard deviations of 0.2 K,

0.4 K, and 0.6 K, respectively.

The RMS error increases as the Gaussian noise increases. However, In Fig. 5a, the RMS error changes very little in the range of 58°~65°. The RMS error of VR first increases and then decreases with increasing incidence angle, and it reaches its minimum and maximum values at 0° and 56°, respectively. The RMS error of HR decreases with increasing incidence angle and reaches its maximum and minimum values at 0° and 65°, respectively. The RMS error of AR first decreases and then increases with increasing incidence angle and reaches its maximum and minimum values at 0° and 59°, respectively. The trend of retrieval accuracy with incidence angle is caused by the sensitivity of brightness temperature to the sea surface wind speed (section 3.1) and the interaction between different channels.

Table 2 shows the maximum and minimum values of RMS error. In general, the retrieval accuracy for HR is higher than that for VR, and the retrieval accuracy achieved using AR is the highest. AR can be used as an SSWS retrieval method for spaceborne one-dimension synthetic aperture radiometer, and it is necessary to retrieve the SSWS at larger incidence angle.

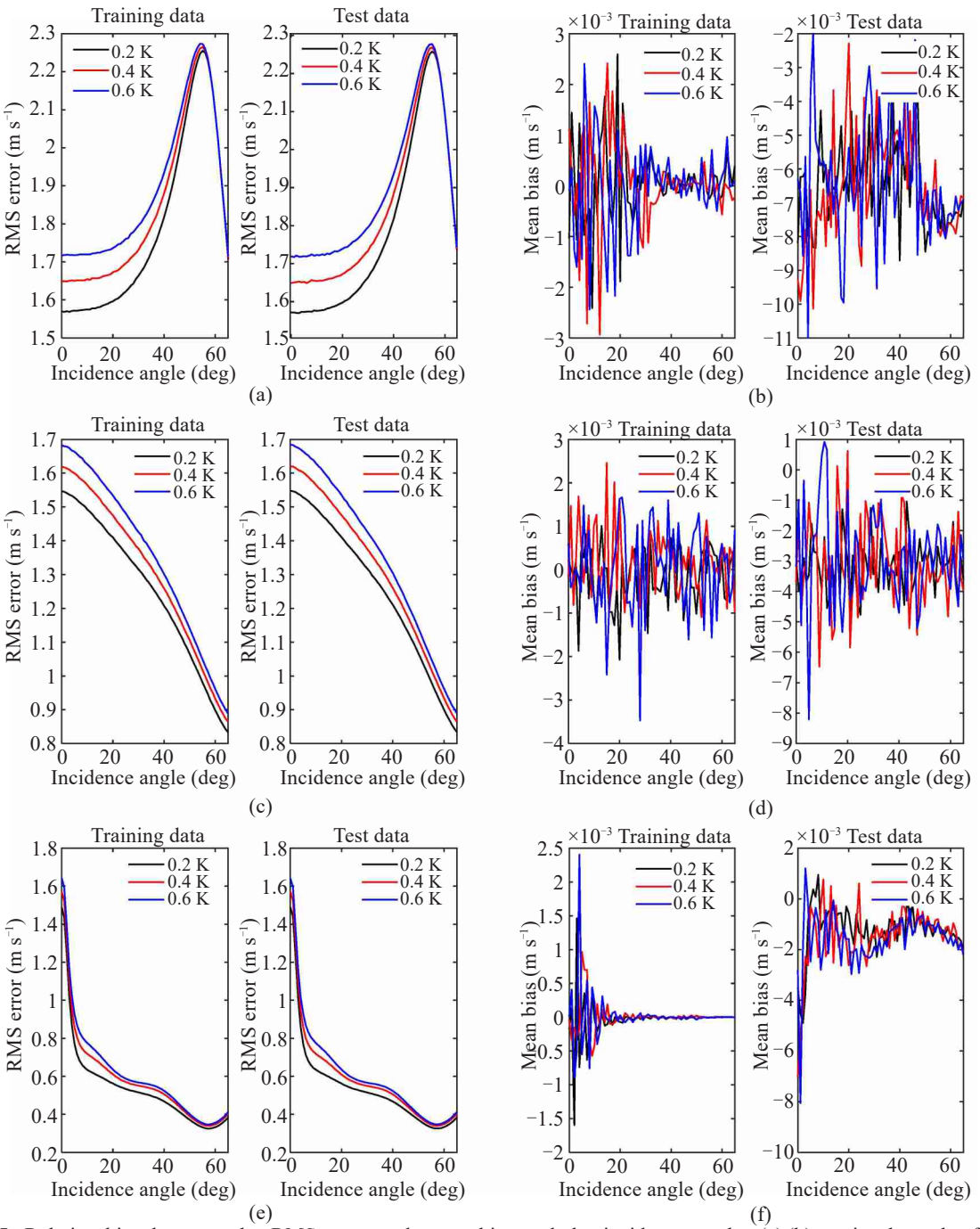

Figure 5. Relationships between the RMS error and mean bias and the incidence angle: (a)(b) retrieval results for vertical polarization channels, (c)(d) retrieval results for horizontal polarization channels, and (e)(f) retrieval results for all channels.

Table 2. The maximum and minimum values of RMS error.

Gaussian noise (K)	VR (m s^{-1})	HR (m s^{-1})	AR (m s^{-1})
0.2 K	1.56 / 2.25	0.83 / 1.54	0.32 / 1.48
0.4 K	1.64 / 2.26	0.86 / 1.61	0.33 / 1.57
0.6 K	1.71 / 2.27	0.89 / 1.68	0.34 / 1.64

4 CONCLUSIONS

In this paper, we proposed an SSWS retrieval method for the multiple incidence angles characteristic of one-dimensional synthetic aperture microwave radiometer. Assuming that a one-dimensional synthetic aperture microwave radiometer operates at various frequencies (i.e., 6.9, 10.65, 18.7, 23.8 and 36.5 GHz), a radiation transmission model was developed to simulate the measured brightness temperature. Then, the sensitivity of the brightness temperature to the SSWS was calculated, and we used vertical polarization channels (VR), horizontal polarization channels (HR) and all channels (AR) to investigate the SSWS retrieval results at the range of 0°~65°. The conclusions are as follows:

The sensitivity of the vertical polarization brightness temperature to the SSWS gradually decreases as the incidence angle increases, but it remains nearly unchanged in the range of 0°~30°. At 6.9 and 10.65 GHz, the horizontal polarization brightness temperatures show a sensitivity to the SSWS that increases as the incidence angle increases. At 18.7, 23.8 and 36.5 GHz, the sensitivity first increases and then decreases with increasing incidence angle. The RMS error of VR, HR and AR change differently with increasing incidence angle. In general, the retrieval accuracy when using AR is the highest and the retrieval accuracy when using only the VR is the lowest.

This algorithm is suitable for sea surface wind speed retrieval under multiple incidence angles, and reveals the variation of sea surface wind speed retrieval accuracy with incidence angle. We suggest that AR can be used to retrieve SSWS by spaceborne one-dimension synthetic aperture radiometer and it necessary to retrieve the SSWS at larger incidence angle. Because it is simple to operate the algorithm, it can be used as a method for on-board processing in the future.

REFERENCES

[1] MEISSNER T, WENTZ F J. Wind-vector retrievals under rain with passive satellite microwave radiometers [J]. IEEE Transactions on Geoscience and Remote Sensing, 2009, 47 (9): 3065-3083, https://doi. org / 10.1109 / TGRS.2009.2027012.

[2] YAO P, WAN J, WANG J, et al. Satellite retrieval of hurricane wind speeds using the AMSR2 microwave radiometer [J]. Chin J Oceanol Limnol, 2015, 33(5): 1104-1114, https://doi.org/10.1007/s00343-015-4131-9.

[3] FANG Jia-bei , YANG Xiu-qun. The role of meridional wind stress in the tropical unstable air-sea interaction [J]. J Trop Meteor, 2003, 9(1): 95-104, https://doi.org/10.3969/j.issn.1006-8775.2003.01.012.

[4] WANG J, ZHANG J, WANG J. Sea surface wind speed retrieval under rain with the HY-2 microwave radiometer [J]. Acta Oceanologica Sinica, 2017, 36(7): 32-38, https://doi.org/10.1007/s13131-017-1080-5.

[5] WU S T, FUNG A K. A noncoherent model for microwave emissions and backscattering from the sea surface [J]. J Geophys Res (1896-1977), 1972, 77(30): 5917-5929, https://doi.org/10.1029/JC077i030p05917.

[6] WENTZ F J. A two-scale scattering model for foam-free sea microwave brightness temperatures [J]. J Geophys Res (1896-1977), 1975, 80(24): 3441-3446, https://doi. org / 10.1029/JC080i024p03441.

[7] MEISSNER T, WENTZ F J. The Emissivity of the Ocean Surface Between 6 and 90 GHz over a large range of wind speeds and earth incidence angles [J]. IEEE Transactions on Geoscience and Remote Sensing, 2012, 50(8): 3004-3026, https://doi.org/10.1109/TGRS.2011.2179662.

[8] WENTZ F J. A model function for ocean microwave brightness temperatures [J]. J Geophys Res: Oceans, 1983, 88(C3): 1892-1908, https://doi. org / 10.1029 / JC088iC03p01892.

[9] HONG S, SHIN I. Wind speed retrieval based on sea surface roughness measurements from spaceborne microwave radiometers [J]. J Applied Meteorol Climatol, 2013, 52(2): 507-516, https://doi. org / 10.1175 / jamc-d-11-0209.1.

[10] VINE D M L, KAO M, SWIFT C T, et al. Initial results in the development of a synthetic aperture microwave radiometer [J]. IEEE Transactions on Geoscience & Remote Sensing, 1990, 28(4): 614-619, https://doi. org / 10.1109/TGRS.1990.572965.

[11] VINE D M L. The sensitivity of synthetic aperture radiometers for remote sensing applications from space [J]. Radio Science, 1990, 25(4): 441-453, https://doi. org / 10.1029/RS025i004p00441.

[12] LI Q, CHEN K, GUO W, et al. An Aperture Synthesis Radiometer Millimeter Wave Band [M]// 2008: 1699-1701.

[13] SCHANDA E. Multiple Wavelength Aperture Synthesis for Passive Sensing of the Earth's Surface [C]// 1979 Antennas and Propagation Society International Symposium, 1979: 762-763.

[14] RUF C S, SWIFT C T, TANNER A B, et al. Interferometric synthetic aperture microwave radiometry for the remote sensing of the Earth [J]. IEEE Transactions on Geoscience and Remote Sensing, 1988, 26(5): 597-611, https://doi.org/10.1109/36.7685.

[15] CHEN K, ZHU Y, GUO X, et al. Design of 8mm-band aperture synthetic radiometer and imaging experiment [J]. Journal of Infrared, Millimeter, and Terahertz Waves, 2010, 31(6): 724-734, https://doi.org/10.1007/s10762-010-9631-2.

[16] FENG M, AI W, CHEN G, et al. A Multiple linear regression algorithm for sea surface temperature retrieval by one-dimensional synthetic aperture microwave radiometry [J]. J Atmos Oceanic Technol, 2020, 37(9): 1753-1761, https://doi.org/10.1175/JTECH-D-20-0003.1.

[17] LI Q, HU F, GUO W, et al. A General Platform for Millimeter Wave Synthetic Aperture Radiometers [C]// IGARSS 2008 - 2008 IEEE International Geoscience and Remote Sensing Symposium, Boston: IEEE, 2008: 1156-1159.

[18] AI W, FENG M, CHEN G, et al. Research on sea surface temperature retrieval by the one-dimensional synthetic aperture microwave radiometer, 1D-SAMR [J]. Acta Oceanologica Sinica, 2020, 39(5): 115-122, https://doi.org/10.1007/s13131-020-1540-1.

[19] BETTENHAUSEN M H, SMITH C K, BEVILACQUA R M, et al. A nonlinear optimization algorithm for WindSat wind vector retrievals [J]. IEEE Transactions on Geoscience and Remote Sensing, 2006, 44(3): 597-610, https://doi.org/10.1109/TGRS.2005.862504.

[20] BROWN S T, RUF C S, LYZENGA D R. An emissivity-based wind vector retrieval algorithm for the WindSat polarimetric radiometer [J]. IEEE Transactions on Geoscience and Remote Sensing, 2006, 44(3): 611-621, https://doi.org/10.1109/TGRS.2005.859351.

[21] KONER P, HARRIS A, MATURI E. A physical deterministic inverse method for operational satellite remote sensing: an application for sea surface temperature retrievals [J]. IEEE Transactions on Geoscience and Remote Sensing, 2015, 53: 1-17, https://doi.org/10.1109/TGRS.2015.2424219.

[22] MEISSNER T, WENTZ F. Ocean retrievals for WindSat: radiative transfer model, algorithm, validation [C]// Proceedings of OCEANS 2005 MTS/IEEE, 2005: 130-133.

[23] WENTZ F J, MEISSNER T. Algorithm Theoretical Basis Document (ATBD) AMSR Ocean algorithm [R]. California: Remote Sensing Systems, 2000.

[24] GOODBERLET M A, SWIFT C T, WILKERSON J C. Ocean surface wind speed measurements of the Special Sensor Microwave / Imager (SSM / I) [J]. IEEE Transactions on Geoscience & Remote Sensing, 1990, 28 (5): 1-828, https://doi.org/10.1109/36.58969.

[25] OBLIGIS E, LABROUE S, AMAR A, et al. Neural networks to retrieve sea surface salinity from SMOS brightness temperatures [C]// IEEE International Geoscience & Remote Sensing Symposium, 2005.

[26] KRASNOPOLSKY V, GEMMILL W, BREAKER L. A neural network multiparameter algorithm for SSM / I ocean retrievals [J]. Remote Sensing of Environment, 2000, 73: 133-142, https://doi.org/10.1016/S0034-4257(00)00088-2.

[27] AN Da-wei, LU Feng, DOU Fang-li, et al. Modeling and quantitative retrieval of finite field for the tropical sea surface wind speed of the fy-3b microwave imager [J]. Journal of Tropical Meteorology, 2015, 21(1): 84-91, https://doi.org/10.16555/j.1006-8775.2015.01.009.

[28] JENA B, SWAIN D, TYAGI A. Application of artificial neural networks for sea-surface wind-speed retrieval from IRS-P4 (MSMR) brightness temperature [J]. IEEE Geoscience & Remote Sensing Letters, 2010, 7(3): 567-571, https://doi.org/10.1109/LGRS.2010.2041632.

[29] ALSWEISS S O, JELENAK Z, CHANG P S. Remote sensing of sea surface temperature using AMSR-2 measurements [J]. IEEE Journal of Selected Topics in Applied Earth Observations and Remote Sensing, 2017, 10(9): 3948-3954, https://doi. org / 10.1109 / JSTARS.2017.2737470.

[30] WANG Jin, ZHANG Jie, FAN Chenqing, et al. A new algorithm for sea-surface wind-speed retrieval based on the L-band radiometer onboard Aquarius [J]. Chinese Journal of Oceanology and Limnology, 2015, 33(5): 1115-1123, https://doi.org/10.1007/s00343-015-4123-9.

[31] SMITH C K, BETTENHAUSEN M, GAISER P W. A statistical approach to WindSat ocean surface wind vector retrieval [J]. IEEE Geoscience and Remote Sensing Letters, 2006, 3(1): 164-168, https://doi. org / 10.1109 / LGRS.2005.860661.

[32] WILHEIT T T, CHANG A T C. An algorithm for retrieval of ocean surface and atmospheric parameters from the observations of the scanning multichannel microwave radiometer [J]. Radio Science, 1980, 15(3): 525-544, https://doi.org/10.1029/RS015i003p00525.

[33] LOJOU J-Y, BERNARD R, EYMARD L. A simple method for testing brightness temperatures from satellite microwave radiometers [J]. Journal of Atmospheric and Oceanic Technology, 1994, 11(2): 387-400, https://doi.org/10.1175/1520-0426(1994)011<0387:asmftb>2.0.co;2.

[34] MILMAN A S, WILHEIT T T. Sea surface temperatures from the scanning multichannel microwave radiometer on Nimbus 7 [J]. Journal of Geophysical Research: Oceans, 1985, 90(C6): 11631-11641, https://doi. org / 10.1029 / JC090iC06p11631.

[35] LI J, PAN Y, CHEN Y, et al. Estimating typhoon waves based on the Modified ECMWF ERA-5 wind data [J]. Journal of Coastal Research, 2020, 95(sp1): 1177, https://doi.org/10.2112/SI95-228.1.

[36] HILBURN K A, MEISSNER T, WENTZ F J, et al. Ocean vector winds from windsat two-look polarimetric radiances [J]. IEEE Transactions on Geoscience and Remote Sensing, 2016, 54(2): 918-931, https://doi. org / 10.1109/TGRS.2015.2469633.

[37] MEISSNER T, WENTZ F J. The complex dielectric constant of pure and sea water from microwave satellite observations [J]. IEEE Transactions on Geoscience and Remote Sensing, 2004, 42(9): 1836-1849, https://doi.org/10.1109/TGRS.2004.831888.

[38] WATERS J W: 2.3. 2-3 Absorption and Emission by Atmospheric Gases [J]. Methods in Experimental Physics, 1976: 142-176, https://doi. org / 10.1016 / S0076-695X(08)60684-5.

[39] WANG Rui, SHI Shun-wen, YAN Wei, et al. Sea surface wind retrieval from polarimetric microwave radiometer in typhoon area [J]. Chinese Journal of Geophysics- Chinese Edition, 2014, 57: 738-751(in Chinese), https://doi. org / 10.6038/cjg20140305.

[40] BOBYLEV L P, ZABOLOTSKIKH E V, MITNIK L M, et al. Atmospheric water vapor and cloud liquid water retrieval over the arctic ocean using satellite passive microwave sensing [J]. IEEE Transactions on Geoscience and Remote Sensing, 2010, 48(1): 283-294, https://doi.org/10.1109/TGRS.2009.2028018.

Citation: AI Wei-hua, FENG Meng-yan, LU Wen, et al. Research on sea surface wind speed retrieval by the one-dimensional synthetic aperture microwave radiometer [J]. J Trop Meteor, 2021, 27(1): 62-69, https://doi.org/10.46267/j.1006-8775.2021.006.